Med Research Open Access

CORRESPONDENCE OPEN ACCESS

Exploring the Potential Anticancer Effects of *Lobelia chinensis* Lour in Liver Cancer via Multiomics Analysis

Zixuan Yang | Li Song | Hongru Chen | Yaoyao Chen | Youyi Xie | Jumin Xie

Hubei Key Laboratory of Renal Disease Occurrence and Intervention, Medical School, Hubei Polytechnic University, Huangshi, Hubei, China

Correspondence: Jumin Xie (xiejumin@hbpu.edu.cn; xiejm922@163.com)

Received: 19 May 2025 | **Revised:** 16 July 2025 | **Accepted:** 22 July 2025

Funding: This study was supported by Key Project in the Scientific Research Plan of the Hubei Province Education Department (D20234505), Open fund research project of Huangshi Key Laboratory of Molecular Diagnosis and Individualized Therapy (FZ2024005), and Open Fund Project of Hubei Key Laboratory for Kidney Disease Pathogenesis and Intervention (2024SJ104).

ABSTRACT

The morbidity and mortality rates of liver cancer have remained high globally, with China reporting the highest number of new cases and deaths. This study aims to explore ingredients with potential for treating liver cancer from LCL and elucidate their underlying molecular mechanisms. A total of 33 effective molecules in LCL were identified from TCM databases, corresponding to 595 target proteins. Additionally, 2384 DEGs associated with liver cancer were obtained from the TCGA database and 1468 from GEO. The analysis identified 56 common targets between LCL and liver cancer, with 5 key targets. Through the liver cancer risk prognosis model, 3 core targets were selected. These core targets were found overexpressed in liver cancer and closely correlated with the high mortality rate of patients. Molecular docking and molecular dynamics simulations confirmed that the 33 components from LCL exhibited strong binding affinity to the 3 core targets. The identified potential drug ingredients in LCL regulate liver cancer cell cycle progression through CCNB1, CCNB2, and CDK1, exerting anticancer effects.

To the Editor, Liver cancer is a deleterious disease that poses a significant threat to human health, accounting for 4.3% of global cancer cases, and 7.8% of all cancer deaths in 2022 [1]. In 2022, China is projected to report approximately 4.8 million new cancer cases and 2.57 million cancer deaths, with around 383,000 of these deaths attributed to liver cancer, representing about half of the world's liver cancer-related deaths [2, 3].

The morbidity and mortality of liver cancer are influenced by multiple factors globally [4]. In developed countries, advancements in medical technology and in-depth research have led to progress in the early diagnosis and treatment of liver cancer, though the outcomes remain unsatisfactory [5, 6]. In developing countries, limited economic resources and medical infrastructure continue to pose significant challenges to liver cancer prevention and treatment [5, 7].

Given these challenges, the search for safe and effective treatments for liver cancer is of utmost importance. Studies have shown that *Lobelia chinensis* Lour (LCL) exhibits strong antitumor activity and plays a critical role in the treatment of hepatocellular carcinoma [8, 9]. The medicinal use of LCL has a long history, with its applications dating back to ancient times for the treatment of snake and insect bites, carbuncles, pustules, severe abdominal edema, and other ailments [10]. Known for its heat-clearing, detoxifying, diuretic, and antiedematous properties, LCL is highly valued in traditional medicine [11].

Given the remarkable pharmacological properties of LCL and its extensive medicinal history, this study aims to investigate the potential therapeutic effects of the bioactive components of LCL on liver cancer using multiomics analysis techniques.

This is an open access article under the terms of the Creative Commons Attribution License, which permits use, distribution and reproduction in any medium, provided the original work is properly cited.

© 2025 The Author(s). *Med Research* published by John Wiley & Sons Australia, Ltd on behalf of Changsha Baiyi Garden Biotechnology Co., LTD.

1 | Potential Anticancer Effects of LCL in Liver Cancer

1.1 | Active Components and Targets of LCL

The active components of LCL were identified using several traditional Chinese medicine databases, including TCMSP, ETCM 2.0, and BATMAN. The SDF format of the component molecules was retrieved from PubChem. Potential targets were predicted using Swiss Target Prediction. All screening criteria were based on our previous publication [12].

Using the screening criteria from the SwissADME website and considering the reliability of target predictions, 33 primary components of LCL were selected (Table S1). After combining the results and eliminating duplicates, a total of 595 predicted targets were identified (Figure 1A, left panel).

1.2 | Liver Cancer Data Acquisition

The dataset GSE84402, comprising 14 liver cancer samples and 14 matched adjacent tissue samples, was obtained from the GEO database. Additionally, transcriptomic data related to liver cancer, which includes 371 tumor samples and 50 normal liver samples, were downloaded from the TCGA database. The transcriptomic and clinical data were integrated, resulting in a cohort of 364 liver cancer cases with comprehensive clinical and molecular profiles.

A total of 19,452 liver cancer-related targets were retrieved from the GeneCards database, from which 3891 targets with a relevance score ≥ 10 were selected. Furthermore, 72 targets were retrieved from the TTD database. A Venn diagram analysis yielded 3927 liver cancer-related targets (Figure 1A, right panel).

1.3 | Identification of Differentially Expressed Genes (DEGs) in Liver Cancer

The GEO microarray data and TCGA data were normalized using R, and DEGs were identified using the "limma" package with Benjamini–Hochberg FDR correction. The screening criteria included a p-value < 0.05 and ($|\log_2$ Fold Change$| > 1$), which were used to identify both upregulated and downregulated genes.

Differential analysis revealed 1468 DEGs, including 940 downregulated and 528 upregulated genes from GEO data. Additionally, 2384 DEGs were identified from TCGA data, with 1556 downregulated and 828 upregulated genes (Figure 1A, right panel).

1.4 | LCL-Liver Cancer Key Target Collection

Liver cancer targets were retrieved from the TTD, GeneCards, GEO, and TCGA databases. Protein–protein interaction (PPI) analysis was conducted using the STRING database to identify key targets involved in LCL-liver cancer. Details referred to Ref. [13].

The predicted targets of the active ingredients in LCL, the DEGs from liver cancer, and liver cancer-related targets were intersected, leading to the identification of 56 common targets (Figure 1A). These 56 LCL-liver cancer intersection targets were then imported into the STRING database for further analysis. PPI analysis primarily based on topological parameters identified 5 key targets: CCNA2, CDK1, CCNB1, CCNB2, and AURKA (Figure 1A).

1.5 | Core Targets Identification

In the TCGA cohort, 364 HCC patients with complete transcriptomic profiles and clinical annotations were randomly stratified into a training set ($n = 256$) and an independent testing set ($n = 108$) using a 7:3 allocation ratio. To evaluate the prognostic relevance of candidate genes in HCC tumorigenesis and progression, univariate Cox regression analysis was conducted on the 5 preidentified key targets within the training cohort.

Prognosis-associated genes were defined as those with a hazard ratio (HR) p-value < 0.05 and subsequently retained for further analysis. To mitigate overfitting, least absolute shrinkage and selection operator (LASSO) regression with 10-fold cross-validation was implemented via the "glmnet" package. Variables penalized by LASSO were incorporated into a multivariate Cox regression model to identify robust core prognostic genes. Details referred to Ref. [13].

Univariate Cox proportional hazards regression analysis was performed on 5 key targets in the TCGA-LIHC cohort using the "survival" package. Four genes exhibited significant associations with overall survival (OS) in HCC (Figure 1B). To mitigate overfitting, these 4 genes were subjected to LASSO regression (Figure 1C and D), followed by multivariate Cox regression. This yielded a prognostic risk model for HCC defined as follows: Risk score (RS) $= 0.4592 \times$ CDK1 $+ 0.5101 \times$ CCNB1 $+ (-0.5986) \times$ CCNB2 (Figure 1E).

1.6 | Cancer Risk Prognostic Model Evaluation

A prognostic risk model was established using core genes identified through stepwise multivariate Cox regression. The risk score (RS) for each patient was calculated using the formula:

$$\mathrm{RS} = \sum \left(\beta_{\mathrm{gene}} \times \mathrm{Expression}_{\mathrm{gene}} \right), \tag{1}$$

where β_{gene} represents the regression coefficient of each prognostic gene, and $\mathrm{Expression}_{\mathrm{gene}}$ denotes its normalized expression level. Patients in the training cohort were stratified into high-risk and low-risk subgroups based on the median RS threshold.

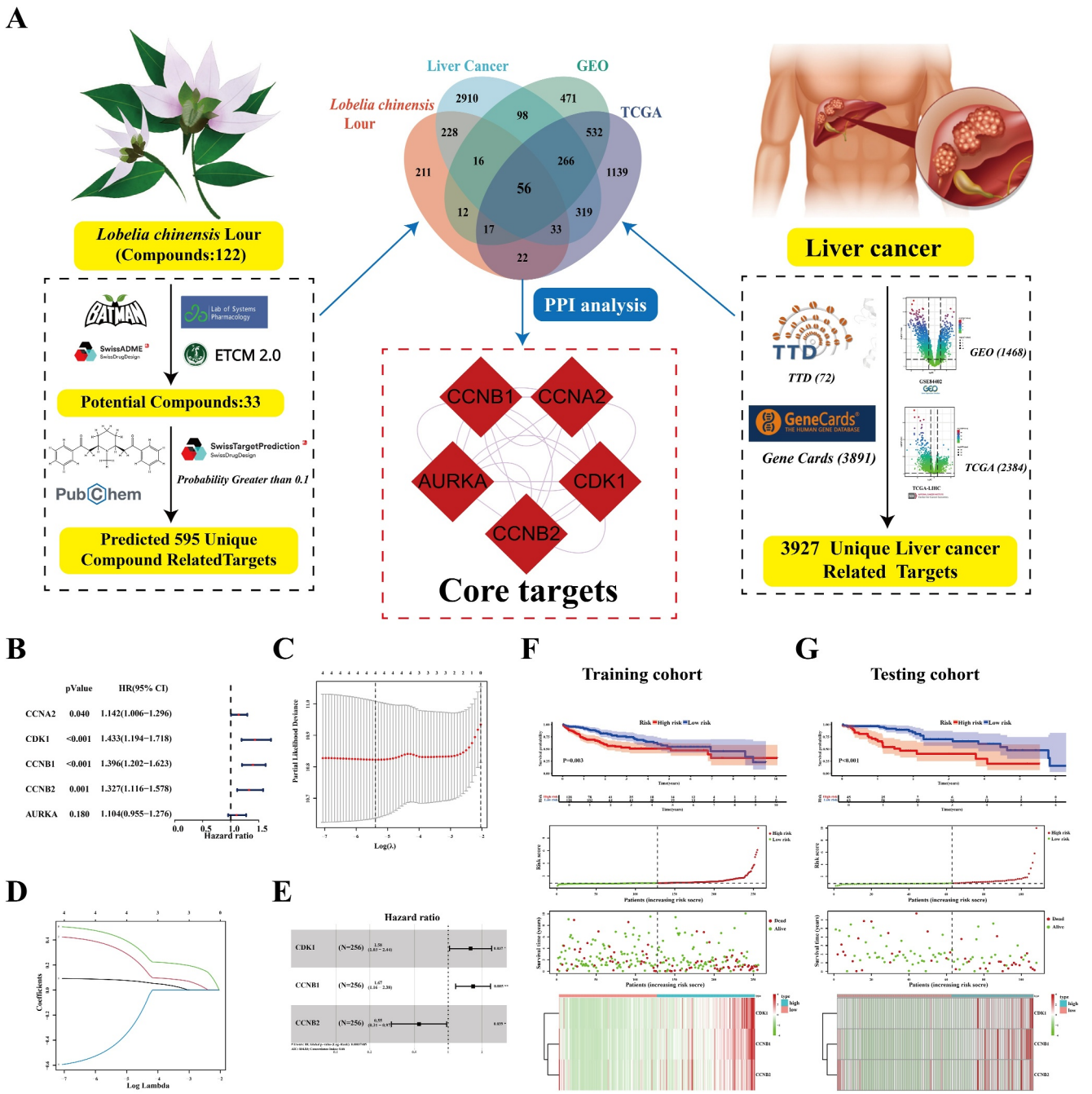


FIGURE 1 | LCL-liver cancer core targets identification. (A) Starting with the compounds from LCL, a series of screening analyses were conducted, integrating liver cancer-related data to identify intersecting targets. A PPI analysis was then performed to determine the key targets. (B) Univariate Cox regression analysis identified 5 prognostic genes ($p < 0.05$). (C) Cross-validation curve of LASSO regression. The dotted line on the left marks the λ value corresponding to the best model fit. (D) Coefficient path diagram of 4 genes, with different-colored lines representing the coefficient changes for each gene. (E) Multivariate Cox regression analysis identified 3 core genes related to prognosis. (F) In the training cohort, KM survival analyses were performed for the high-risk and low-risk groups. The low-risk and high-risk groups were delineated by dotted lines. (G) In the testing cohort, the survival analysis and associated displays were repeated, with the dotted line again used to define the high-risk and low-risk groups.

Kaplan–Meier (KM) survival curves were generated using the R packages "survival" and "survminer", with log-rank tests applied to assess survival differences between subgroups.

To visualize risk stratification, patients were rank-ordered by RS and plots were generated to integrate risk score distribution, survival status, follow-up duration, and prognostic gene expression patterns. This multimodal visualization enabled systematic evaluation of the model's clinical relevance. Details referred to Ref. [13].

Stratification by median RS in the training cohort revealed significantly prolonged OS in low-risk versus high-risk patients. Ordered by ascending RS, RS distribution plots showed: (1)

Positive correlation between RS and expression of CDK1, CCNB1, and CCNB2, (2) inverse correlation between RS and patient survival time, and (3) increased mortality in high-risk patients, with concordant trends across training and testing cohorts (Figure 1F and G).

1.7 | Core Targets Validation

Molecular docking and dynamics simulations were performed to validate the interactions between active ingredients and the core targets. All setups, details, and procedures were based on our previous study [13]. Additionally, 2D molecular docking interactions were analyzed using the PROTEINS PLUS web tool (https://proteins.plus/).

The binding modes, hydrogen-bond interactions, and key interacting residues between the active components of LCL and the core targets were visualized in both 2D and 3D representations. Asiatic Acid formed two hydrogen bonds with CCNB1 at residues LYS-33 (2.0 Å) and ASP-86 (2.5 Å). Lobelanine bound to CCNB2 via hydrogen bonds at residues LYS-349 (2.6 Å) and ASP-297 (3.6 Å). Lobeline established three hydrogen bonds with CDK1 at residues GLU-1608 (2.4 Å), GLN-1615 (3.3 Å), and ARG-1469 (2.9 Å) (Figure 2A). The calculated

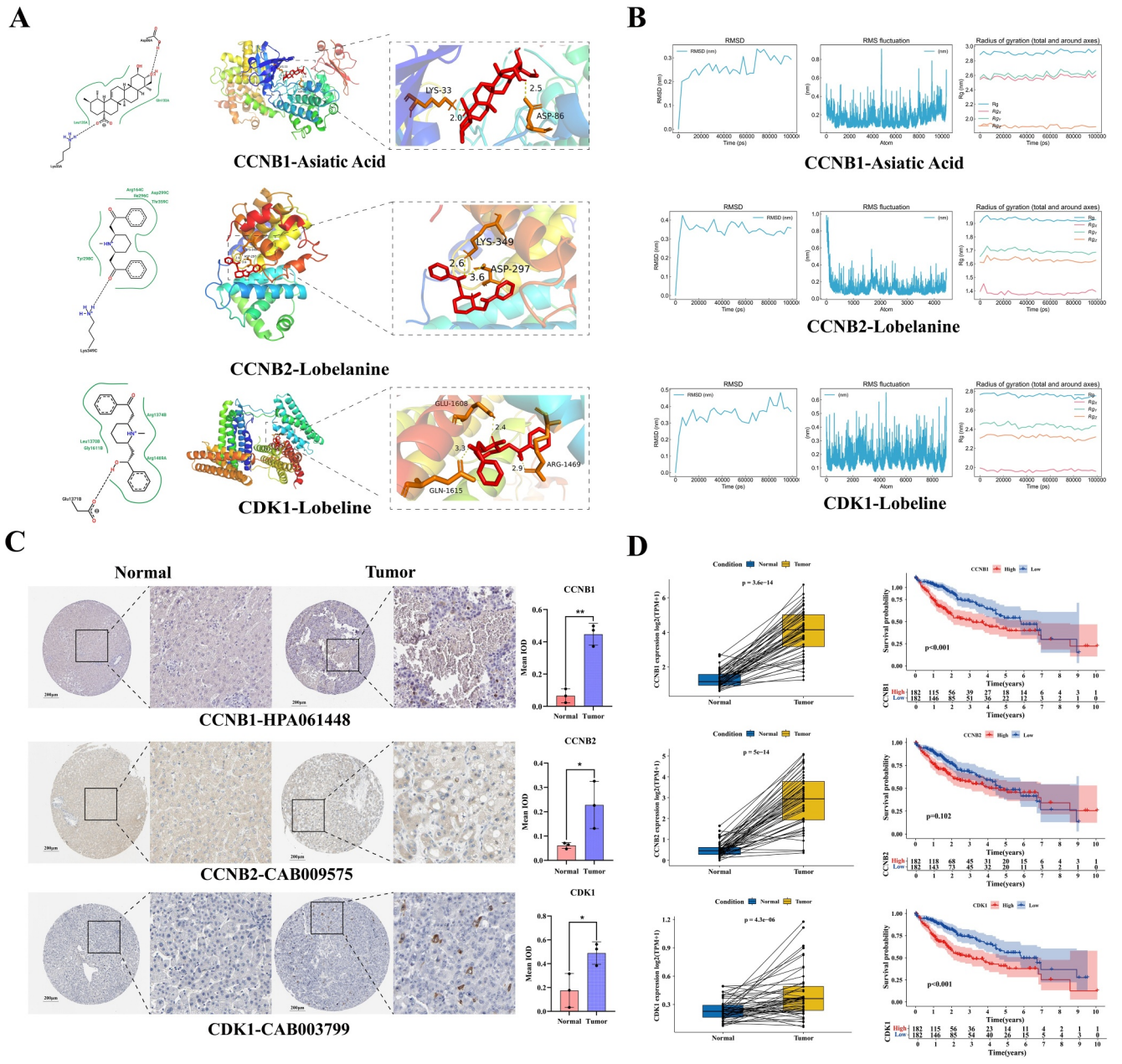


FIGURE 2 | Validation of core targets. (A) 2D and 3D molecular docking structure diagrams of CCNB1, CCNB2, and CDK1 with their respective active compounds. Yellow dashed lines represent hydrogen bonds, and the small molecules are Asiatic Acid, Lobelanine, and Lobeline, respectively. (B) RMSD, RMSF, and RG of CCNB1-Asiatic Acid, CCNB2-Lobelanine, and CDK1-Lobeline. (C) Immunohistochemical staining of CCNB1, CCNB2, and CDK1 proteins in LIHC and normal liver tissues. (D) Differential expression analysis of CCNB1, CCNB2, and CDK1 in LIHC versus paired normal liver tissues. Association of CCNB1, CCNB2, and CDK1 protein expression with prognosis in patients with liver cancer.

binding energies for these complexes were as follows: CCNB1-Asiatic Acid: −9.7 kcal/mol, CCNB2-Lobelanine: −7.6 kcal/mol, and CDK1-Lobeline: −8.3 kcal/mol. These results indicate strong binding affinities.

To validate the docking results, MD simulations were conducted for these complexes. Collectively, the MD simulations corroborated the binding efficacy of Asiatic Acid-CCNB1, Lobelanine-CCNB2, and Lobeline-CDK1, supporting their potential as stable complexes (Figure 2B).

The expression profiles of core targets in HCC were analyzed using the Human Protein Atlas (HPA) database to compare protein localization and abundance between tumor tissues and normal tissues [14]. The stained area was quantified using the ImageJ Pro Plus 6 software and statistically analyzed with the GraphPad Prism 8.0 software.

Immunohistochemistry (IHC) data for CCNB1, CCNB2, and CDK1 in HCC and normal liver tissues were retrieved from the HPA database using antibodies HPA061448, CAB009575, and CAB003799, respectively. IHC staining revealed markedly elevated protein expression of all three core targets in HCC tissues compared to normal controls (Figure 2C).

RNA sequencing data from the TCGA-LIHC cohort, comprising 49 paired HCC tumors and adjacent nontumorous tissues, were processed using R. Differential expression analysis of core targets was visualized through paired boxplots. Prognostic significance was evaluated via KM survival curves generated with the "survival" package, and statistical validity was assessed using log-rank tests.

Paired mRNA expression analysis demonstrated significantly upregulated CCNB1, CCNB2, and CDK1 transcript levels in tumors ($p < 0.001$). KM survival analysis showed that high CCNB1 and CDK1 expression correlated with increased prognostic hazard, significantly shortening overall survival For CCNB1, this association plateaued after 6 years ($p > 0.05$), likely due to reduced statistical power from limited long-term follow-up. Conversely, CCNB2 exhibited a biphasic survival impact: high expression predicted poorer 5-year OS ($p < 0.05$) but conferred protective effects beyond 5 years, suggesting time-dependent regulatory roles in HCC progression (Figure 2D).

2 | Conclusion

CDK1 is a crucial cell cycle protein kinase and a key regulator of cell cycle progression. Its primary function involves forming a cyclin-dependent kinase complex with cyclins (CCNB1/2), thereby regulating cell cycle progression [15].

High expression of CCNB1, CCNB2, and CDK1 suggests that these genes may play critical roles in the onset and progression of liver cancer. Their upregulation may be associated with the proliferation, malignant transformation, and aggressiveness of liver cancer cells [16]. Therefore, these genes not only serve as potential diagnostic markers for liver cancer but may also become novel therapeutic targets, offering new strategies for early diagnosis and treatment. Survival curve analysis indicated that elevated expression of CCNB1, CCNB2, and CDK1 increased the risk of mortality in patients with liver cancer.

Compared to existing CDK1 inhibitors and approved targeted therapies for liver cancer (e.g., sorafenib and regorafenib), it remains uncertain whether the LCL components provide advantages in terms of pharmacodynamics, toxicity, or side effects. The limitations of this study are as follows: (1) Computational predictions require experimental validation of binding and function, (2) the prognostic model lacks external validation, and (3) the pharmacokinetic/pharmacodynamic properties of the LCL components were not assessed.

This study employed multiomics analysis to explore key drug molecules in LCL with potential antiliver cancer effects. These molecules, including Asiatic Acid, Lobelanine, and Lobeline, probably regulate the expression of CCNB1, CCNB2, and CDK1, thereby exerting the inhibition of liver cancer progression.

Acknowledgments

This study was supported by Key Project in the Scientific Research Plan of the Hubei Province Education Department (D20234505), Open fund research project of Huangshi Key Laboratory of Molecular Diagnosis and Individualized Therapy (FZ2024005), and Open Fund Project of Hubei Key Laboratory for Kidney Disease Pathogenesis and Intervention (2024SJ104).

Conflicts of Interest

The authors declare no conflicts of interest.

Zixuan Yang
Li Song
Hongru Chen
Yaoyao Chen
Youyi Xie
Jumin Xie

References

1. F. Bray, M. Laversanne, H. Sung, et al., "Global Cancer Statistics 2022: GLOBOCAN Estimates of Incidence and Mortality Worldwide for 36 Cancers in 185 Countries," *CA: A Cancer Journal for Clinicians* 74, no. 3 (2024): 229–263, https://doi.org/10.3322/caac.21834.

2. B. Han, R. Zheng, H. Zeng, et al., "Cancer Incidence and Mortality in China, 2022," *Journal of the National Cancer Center* 4, no. 1 (2024): 47–53, https://doi.org/10.1016/j.jncc.2024.01.006.

3. Liver Cancer Statistics. (2024), https://www.wcrf.org/preventing-cancer/cancer-statistics/liver-cancer-statistics/.

4. E. Y. Tan, P. Danpanichkul, J. N. Yong, et al., "Liver Cancer in 2021: Global Burden of Disease Study," *Journal of Hepatology* 82, no. 5 (2024): 851–860, https://doi.org/10.1016/j.jhep.2024.10.031.

5. J. D. Yang, P. Hainaut, G. J. Gores, A. Amadou, A. Plymoth, and L. R. Roberts, "A Global View of Hepatocellular Carcinoma: Trends, Risk, Prevention and Management," *Nature Reviews Gastroenterology & Hepatology* 16, no. 10 (2019): 589–604, https://doi.org/10.1038/s41575-019-0186-y.

6. H. Rumgay, M. Arnold, J. Ferlay, et al., "Global Burden of Primary Liver Cancer in 2020 and Predictions to 2040," *Journal of Hepatology* 77, no. 6 (2022): 1598–1606, https://doi.org/10.1016/j.jhep.2022.08.021.

7. T. Akinyemiju, S. Abera, M. Ahmed, et al., "The Burden of Primary Liver Cancer and Underlying Etiologies From 1990 to 2015 at the Global, Regional, and National Level: Results From the Global Burden of Disease Study 2015," *JAMA Oncology* 3, no. 12 (2017): 1683–1691, https://doi.org/10.1001/jamaoncol.2017.3055.

8. J. Luo, Qx Chen, P. Li, et al., "Lobelia chinensis Lour Inhibits the Progression of Hepatocellular Carcinoma via the Regulation of the PTEN/AKT Signaling Pathway in Vivo and in Vitro," *Journal of Ethnopharmacology* 318, no. Pt A (2024): 116886, https://doi.org/10.1016/j.jep.2023.116886.

9. M. W. Chen, W. R. Chen, J. M. Zhang, X. Y. Long, and Y. T. Wang, "Lobelia Chinensis: Chemical Constituents and Anticancer Activity Perspective," *Chinese Journal of Natural Medicines* 12, no. 2 (2014): 103–107, https://doi.org/10.1016/s1875-5364(14)60016-9.

10. J. L. Tang, B. Y. Liu, and K. W. Ma, "Traditional Chinese Medicine," *Lancet* 372, no. 9654 (2008): 1938–1940, https://doi.org/10.1016/s0140-6736(08)61354-9.

11. K. C. Li, Y. L. Ho, G. J. Huang, and Y. S. Chang, "Anti-Oxidative and Anti-Inflammatory Effects of Lobelia chinensis in Vitro and in Vivo," *American Journal of Chinese Medicine* 43, no. 2 (2015): 269–287, https://doi.org/10.1142/s0192415x15500184.

12. J. Xie, Y. Zhu, H. Bai, et al., "Multi-Omics Analysis of the Anti-Cancer Effects of Curcumol in Endometrial Carcinoma," *Frontiers in Pharmacology* 16 (2025): 16–2025, https://doi.org/10.3389/fphar.2025.1565959.

13. J. Xie, Y. Zhu, Z. Yang, Z. Yu, M. Yang, and Q. Wang, "An Integrative Analysis Reveals Cancer Risk Associated With Artificial Sweeteners," *Journal of Translational Medicine* 23, no. 1 (2025): 32, https://doi.org/10.1186/s12967-024-06047-0.

14. M. Uhlén, et al., "Proteomics. Tissue-Based Map of the Human Proteome," *Science* 347, no. 6220 (2015): 1260419.

15. I. Pellarin, A. Dall'Acqua, A. Favero, et al., "Cyclin-Dependent Protein Kinases and Cell Cycle Regulation in Biology and Disease," *Signal Transduction and Targeted Therapy* 10, no. 1 (2025): 11, https://doi.org/10.1038/s41392-024-02080-z.

16. N. Li, Y. Zheng, J. Xu, et al., "Squid-Derived Protamine: A Natural Basic Protein and Its Pegylated Derivative as Anti-Cancer Agents in Hepatocellular Carcinoma," *International Journal of Biological Macromolecules* 318, no. Pt 3 (2025): 145044, https://doi.org/10.1016/j.ijbiomac.2025.145044.

Supporting Information

Additional supporting information can be found online in the Supporting Information section.